Quantitative analysis of the regulation of leukocyte chemosensory migration by a vascular prosthetic biomaterial

C. C. CHANG, S. M. LIEBERMAN, P. V. MOGHE*
Department of Chemical and Biochemical Engineering, Rutgers University, Piscataway, NJ 08854–8058, USA
E-mail: moghe@rci.rutgers.edu

The need for improved, infection-resistant vascular biomaterials calls for more objective evaluation of the immune pathophysiology of implantable prosthetic materials. In this study we have developed a new strategy to quantitatively characterize population-averaged responses of immune cell migration on vascular prosthetic materials. This approach, incorporating a chemokinetically regulated ''biomaterial-gel'' sandwich configuration, was applied to quantify both random and directed modes of the chemosensory migration of human neutrophil leukocytes on expanded polytetrafluoroethylene (ePTFE). Our studies show that (a) microporous, synthetic materials like ePTFE suppress the basal rate of random cell migration relative to that reported on non-porous control surfaces; (b) stimulation with chemoattractant (formyl peptide) can significantly elevate rates of random and directed migration on ePTFE; and (c) protein conditioning of ePTFE with albumin or immunoglobulin G can differentially modulate the rates and relative proportion of random and directional components of leukocyte migration response to chemoattractant. This, to our knowledge, is the first objective quantitation of chemokinetically regulated cell migration on implantable prosthetic materials.

1. Introduction

The reconstruction of blood vessels using synthetic biomaterials can fail due to uncontrolled bacterial infection. It has been well established that the presence of a foreign body in the tissue, such as an implanted device, increases the risk of infection [1–3]. Once infected, synthetic vascular grafts have been shown to exhibit a steady colonization of graft interstices by bacteria, a process that is initiated early on, and may persist over long periods of time [4]. Anticoagulant and antiplatelet activation therapy have proven to be ineffective in the prevention of infection and thrombosis on vascular biomaterials [5]. In an attempt to understand the origin of periprosthetic infection, several studies have focused on the role of polymorphonuclear leukocytes, the primary white blood cells that launch the host acute inflammatory response following infection [6–9]. It has been proposed that prosthetic biomaterials may cause an impairment in leukocyte functions, leading to impaired host defense in the region of the implant [10].

The presence of vascular prosthetic materials has been found to cause leukocyte activation both *in vivo*, during cardio-pulmonary bypass [11] and hemodialysis [12], and *in vitro* [13], although there is no unequivocal evidence yet of the diminished leukocyte reactivity caused by these materials. Another likely function of leukocytes that may be impaired on prosthetic materials, is migration, since migration is critical for polymorphonuclear neutrophilic leukocytes (PMNs) adherent to luminal implant surfaces to navigate toward sites of infection. However, the sensitivity of leukocyte migration to vascular biomaterials *in vitro* has been extremely difficult to examine directly.

Typical *in vitro* assays to assess leukocyte migratory response to prosthetic biomaterials have traditionally involved three steps [14], first, cellular ''priming'' through brief co-incubation with the relevant material, followed by cell detachment, and finally, the study of the migration of primed cells in an *ex situ* migration chamber. The pitfalls of these methods are that: (i) they assess only indirect, often transient secondary effects of biomaterial stimulation on leukocyte migratory behavior; (ii) they cannot evaluate migratory responses to physiologic modifications in vascular prosthetic material; including the effect of biochemical stimulation, or of the material chemistry and microstructure; and (iii) the measured migration response may, in fact, be artifactual and biased by the substrate configuration used in the

*Author to whom all correspondence should be addressed.

migration chamber. Thus, there is a critical need for techniques permitting direct evaluation of the extent and mode of blood cell migration on vascular biomaterials.

To that end, this paper concerns the development of a new assay to quantitatively evaluate leukocyte migratory behavior on prosthetic biomaterial surfaces. Our assay utilizes a ''biomaterial-cell-gel'' sandwich configuration, wherein cellular migration is allowed to proceed directly within the region between a prosthetic biomaterial membrane (typically, microporous) and an overlaid composite gel. Similar confined configurations have been used previously on smooth, two-dimensional tissue culture surfaces, to study population cell migration under agarose [15–17]. The major advantage of such assays is that the gel matrix allows the incorporation of soluble chemotactic factors, whose effect on chemosensory migration can be tested *in situ*.

Based on the new migration assay, we have investigated the effect of stimulation by the chemotactic peptide, N-formyl-methionyl-leucyl-phenylalanine (FMLP), on the migratory behavior of human PMN adherent to the prosthetic biomaterial, expanded polytetrafluoroethlylene (ePTFE). The extent of leukocyte population migratory behavior was quantified in terms of indices for random migration (in response to uniform chemoattractant concentration) and chemotaxis (in response to chemoattractant concentration gradient). Additionally, we have evaluated chemosensory migration in response to surface adsorption on ePTFE of two major plasma proteins [18], albumin and IgG. These studies reveal insights into the potential control of PMN migration behavior on physiologically conditioned biomaterials. We report that the rate of leukocyte migration on native prosthetic materials such as ePTFE was greatly reduced in the absence of chemotactic factors, but that this migration was highly activatable by chemotactic stimulation. Further, we demonstrate that both random and chemotactic modes of leukocyte chemosensory migration on ePTFE were differentially regulated by the nature of adsorbed proteins.

2. Materials and methods

2.1. Pretreatment of biomaterial

Expanded PTFE with uniform 30 μm internodal distance was generously donated by W. L. Gore and Associates, Inc. (Flagstaff, AZ, USA). Rectangular segments (45×35 mm) of ePTFE were affixed to the bottom of 60×15 mm tissue culture dishes with a smear of inert silicon vacuum gel. The biomaterial was then incubated overnight (for at least 8 h) with 6 ml of various plasma protein solution in order to coat the surface of the biomaterial. The specific plasma proteins studied were human serum albumin (HSA) and immunoglobulin G (IgG). For albumin coated surfaces, the biomaterial was incubated with a 5% HSA solution in Hanks' Balanced Salt Solution (HBSS). As for IgG coated surfaces, 5 mg/ml of stock solution was diluted to a concentration of 50 μg/ml in HBSS. The untreated, or native, control sample was incubated in HBSS. After pretreatment, the samples were washed with HBSS three times to remove any unadsorbed protein.

2.2. Leukocyte isolation

Fifty milliliters of blood was typically drawn from healthy volunteer donors in accordance with the protocols established by the Rutgers University Institutional Review Board. Polymorphonuclear leukocytes (PMN, or neutrophils) were isolated by the single step density gradient centrifugation using a modification of Boyum's technique [19]. Briefly, the blood was layered on top of ''neutrophil isolation media'' (NIM) (Cardinal Associates) (2 volumes blood with 1 volume NIM) and centrifuged at 1380 rpm for 30 min at room temperature. The PMN-rich layer was aspirated, washed, and centrifuged with HBSS without calcium and magnesium. In order to sediment the red blood cells, the PMN pellet was then diluted in E-LYSE and centrifuged at 1000 rpm for 10 min. The PMN pellet was then re-suspended in HBSS at a concentration of 30×10^6 cells/ml (twice the desired final concentration). More than 95% PMNs were tested to be viable using tryspan/blue exclusion.

2.3. Preparation of chemotactic factor

FMLP (MW: 437.6), was prepared as a stock solution 5×10^{-3} M (in sterile DMSO), frozen in 15 μl aliquots at -80 °C and then thawed and diluted as required for the experiments.

2.4. Preparation of gelatin-agarose composite gel

Bovine gelatin (Sigma) was dissolved in 2X Minimum Essential Medium (MEM) at 60 °C at a concentration of 1% w/v and a pH of 7.5. Indubiose A37 agarose (Biosepra) was dissolved in boiling distilled water at a concentration of 2% w/v. The agarose solution was cooled in 60 °C water bath and combined with an equal volume of the gelatin solution to achieve final concentrations of 1% w/v agarose and 0.5% w/v gelatin. The combined solution (with various concentrations of FMLP for studies on random migration; without FMLP for studies on chemotaxis) was first cooled to 40 °C to prevent denaturation of the protein coating and FMLP, and then added to the chamber workspace so as to yield a uniform height of 3 mm for the agarose gel. The chambers with gelled gel were refrigerated 30 min prior to use.

2.5. Preparation of migration chamber

The migration chamber was adapted from a previously published prototype for a linear under-agarose chamber [20].

Random migration assay. A 2.4×39 mm linear ''cell well'' was cut approximately at the center of the gelled chamber using previously fabricated plexiglass templates to ensure reproducibility, and the segments of gel gently removed with a hypodermic syringe (aspiration was not used since it was found to be disruptive). The cell suspension made up in the appropriate concentration of FMLP was then added to the cell well. The plates were incubated at 37 °C in a 5% CO_2 water-jacketed incubator for 3 h.

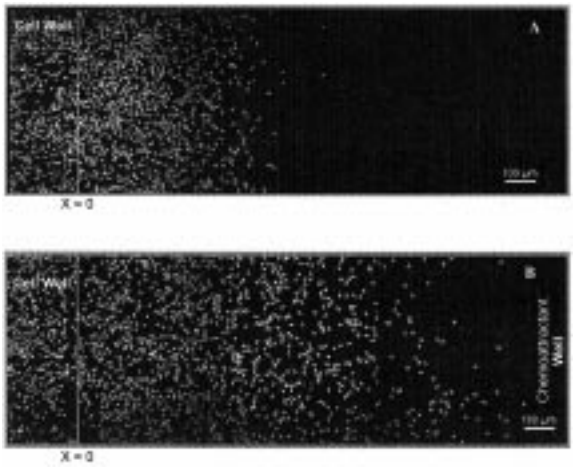

Figure 1 (A): Confocal micrograph of leukocyte migration on native ePTFE in the presence of uniform concentration of FMLP (10^{-8} M). (B): Confocal micrograph of leukocyte migration along FMLP concentration gradient, which was established from the chemoattractant well to the right. Both patterns A and B were obtained after incubating $\sim 2.5 \times 10^6$ PMN in the cell well for 3 h. In B, the chemoattractant well was spaced 5 mm from the cell well and loaded with 1×10^{-7} M FMLP. $X = 0$ indicates the cell well boundary.

Chemotaxis assay. Using prefabricated templates, two linear wells (2.4×39 mm), 5 mm apart, were cut in the gelled chamber, the center one as the cell well and the peripheral one serving as the chemoattractant well (Fig. 1b). Gel in the attractant well was then removed, agarose/gelatin solution containing FMLP (10^{-7} M) was added to the height of the adjacent gel slab ($\sim 200\,\mu$l) which separates the cell and attractant wells, and allowed to gel (~ 60 s). The gel in the cell well was removed immediately before the addition of cell suspension without FMLP to minimize the loss of media in the ''sandwich region'' space. The chambers were then further incubated as described for random migration studies.

2.6. Fixation and labeling of migrated PMN

At the end of the incubation period, the cell wells were fixed with the gel in place by flooding the plates with 3 ml of 2.5% glutaraldehyde solution. After 8 h of fixation at 4 °C, the gel layer was carefully removed; the plates were washed gently with 6 ml HBSS three times. Next, Triton X at 0.1% solution was incubated to permeabilize PMN at room temperature for 5 min. Finally, the cell layer was labeled with 2 μM solution of the DNA binding fluorophore, ethidium homodimer-2 (Molecular Probes), in HBSS for 30 min at room temperature and then washed with HBSS three times, before imaging and quantitative analysis.

2.7. Image analysis

Population level cell migration on ePTFE was quantified by measuring time variant and space dependent profiles of cell density, $c(z, t)$, i.e. cell number versus distance migrated outward from the cell well boundary, and substituting these into a theoretical continuum transport model to obtain values of intrinsic population-averaged coefficients, μ and χ. To this end, for every time point, images of regions $50\,\mu\text{m} \times 100\,\mu\text{m}$ were acquired at 50 μm increments along the linear dimension of chamber under fluorescence mode on a Zeiss LSM 410 confocal microscope. The microscope motorized stage enabled the slide to be moved precise increments for an accurate manual measurement of cell number.

2.8. Mathematical analysis to obtain coefficients of cell migration on the biomaterial

The general migration coefficients appear in the following expression for the population cell transport rate, J_c [21]

$$J_c = -\mu(a)\frac{\partial c}{\partial x} + \left[-\frac{1}{2}\frac{d\mu(a)}{da} + \chi(a)\right]\frac{\partial a}{\partial x}c \qquad (1)$$

where c is the cell density and a is the attractant concentration. The random migration coefficient, μ, (units: cm^2/s) and the chemotaxis coefficient, χ, (units: $\text{cm}^2/\text{s} - \text{M}$) characterize the diffusive and vectorial components of migration. The first term on the right hand side of Equation 1 represents the random migration of a cell population on a biomaterial, in the presence of uniform concentration of chemoattractant. The second and third terms represent chemokinesis and chemotaxis respectively, when a spatial attractant gradient, $\partial a/\partial x$, exists.

Random migration characterization: In the absence of FMLP gradient, the expression for J_c in Equation 1 simplifies considerably to a partial differential equation, with the random migration coefficient $\mu(a)$ as an unknown constant.

$$\frac{\partial c}{\partial t} = \mu(a)\frac{\partial^2 c}{\partial x^2} \qquad (2)$$

Equation 2 is solved using the associated boundary conditions

$$\text{c}(0,\ \text{t}) = c_0, t > 0 \qquad (3)$$

$$c(x,\ t) \to 0, x \to \infty$$

Equation 3 means that cells migrating outward from the cell well are continually replenished and that over the time period of our studies, cells do not migrate to the extremities of the chamber.

The solution to Equation 2 is

$$\frac{c}{c_0} = erfc\left[\frac{x}{(4\mu t)^{1/2}}\right] \qquad (4)$$

where x is the distance from the cell well boundary, t is the incubation time, and *erfc* is the complementary error function [22]. $\mu(a)$ is then estimated by using non-linear least square regression on experimental cell density data.

Chemotaxis characterization: The mathematical model for cell migration in a gradient of FMLP is formulated in terms of the expression in Equation 1. Both cell migration and chemoattractant diffusion are modeled, as shown in Equations 5 and 6, respectively

$$\frac{\partial c}{\partial t} = \frac{\partial}{\partial x}\left[\mu(a)\frac{\partial c}{\partial x}\right] - \frac{\partial}{\partial x}\left\{\left[-\frac{1}{2}\frac{d\mu(a)}{da} + \chi(a)\right]\frac{\partial a}{\partial x}c\right\} \quad (5)$$

$$\frac{\partial c}{\partial t} = D\frac{\partial^2 a}{\partial x^2} \quad (6)$$

boundary conditions:

$$x = 0: \quad c = c_0, \quad x = \mathrm{L}: \quad a = a_0,$$

$$x \to \infty: \quad c \to 0, \quad x \to -\infty: \quad a \to 0$$

where L is the distance between the cell well and the chemoattractant well.

The solution to Equation 6 was analogously formulated as the expression in Equation 4. The spatial variation in a and its derivative $\partial a/\partial x$ were determined at various times, and substituted into Equation 5. The numerical solution to Equation 5 was then accomplished in terms of Crank-Nicholson finite difference approximation [23], using Maple V (Version 4) on a Power Macintosh 7500 computer.

2.9. Statistical analysis

Statistical analyzes were performed using unpaired t-test and ANOVA, and a confidence level of 95% ($p < 0.05$) was considered necessary for statistical significance. The error bars indicate the standard error around the average value.

3. Results

3.1. Chemoattractant dependence of leukocyte random migration on ePTFE

A representative confocal fluorescence micrograph of FMLP-induced population-level leukocyte migration outward from the cell well on ePTFE appears in Fig. 1a. Experimental cell density profiles for random migration on native ePTFE are shown in Fig. 2 for three different values of FMLP concentration, after 3 h of incubation on ePTFE. The qualitative nature of the cell density profiles is in good agreement with that of the theoretical model predictions (shown as fitted curves). Corresponding to each of these profiles, therefore, a value for μ, the random migration coefficient, was obtained for every chemoattractant concentration using Equation 4. Values of μ averaged over multiple experiments were plotted versus FMLP concentration (Fig. 3). We observe that the cell population on ePTFE shows an order of magnitude increase in the value of μ over the FMLP concentrations studied. The μ profile had a biphasic nature, with an intermediate FMLP concentration associated with the maximum value for μ. The maximum value of μ on ePTFE surface was $1.09 \times 10^{-7}\,\mathrm{cm}^2/\mathrm{s}$, which occurred at a concentration of about 1×10^{-8} M FMLP.

3.2. Chemoattractant dependence of leukocyte chemotaxis on ePTFE

A typical pattern of leukocyte migration on ePTFE in response to a concentration gradient of FMLP is illustrated by the confocal fluorescence micrograph in Fig. 1B. It is apparent when the migratory behavior in Fig. 1A and B is compared that the extent of leukocyte migration on ePTFE directed by FMLP gradient is significantly greater than observed under a uniform field of an ''optimal'' chemoattractant concentration.

Since FMLP concentration evolved during the course of the chemotaxis experiments, the leukocyte migratory response was studied as a function of both space and time. Representative plots of the experimental and predicted cell density profiles for chemotaxis experiments on native ePTFE were plotted in Fig. 4 for three different periods of incubation time. With each hour increment of time, the distance migrated by cell population was found to approximately double (from $x/L = 0.055$ to 0.11 to 0.205). For each of these cell density profiles, the theoretically predicted profiles (dashed curve) were drawn corresponding to the average χ value for the range of distance traveled by the cell population at each particular time interval. The underlying assumption was that χ was relatively constant for

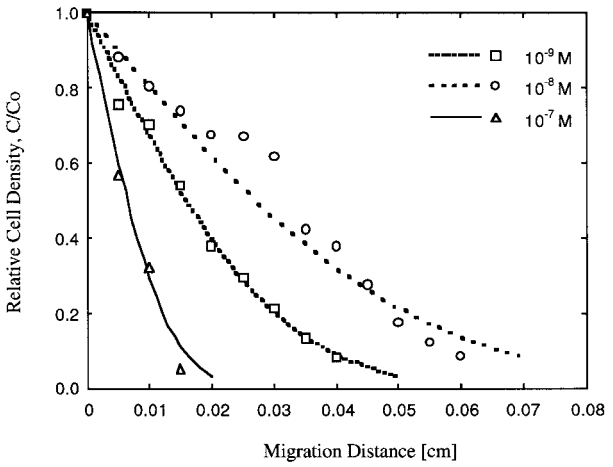

Figure 2 Representative density profiles for leukocytes exhibiting random migration on ePTFE following 3 h incubation with three different concentrations of FMLP. Values of cell density (C) were normalized to those observed at the cell well boundary (C_o). The migration distance was measured outwards from the boundary of the cell well.

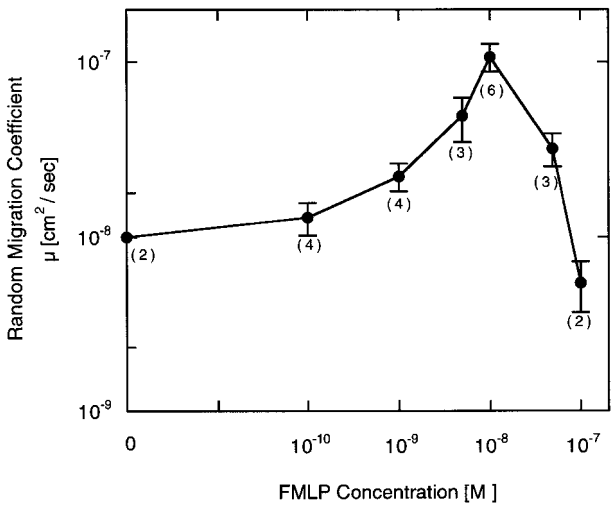

Figure 3 FMLP concentration dependence of μ, the random migration coefficient, of leukocytes adherent to ePTFE. The error bars represent standard error based on the number of trials indicated.

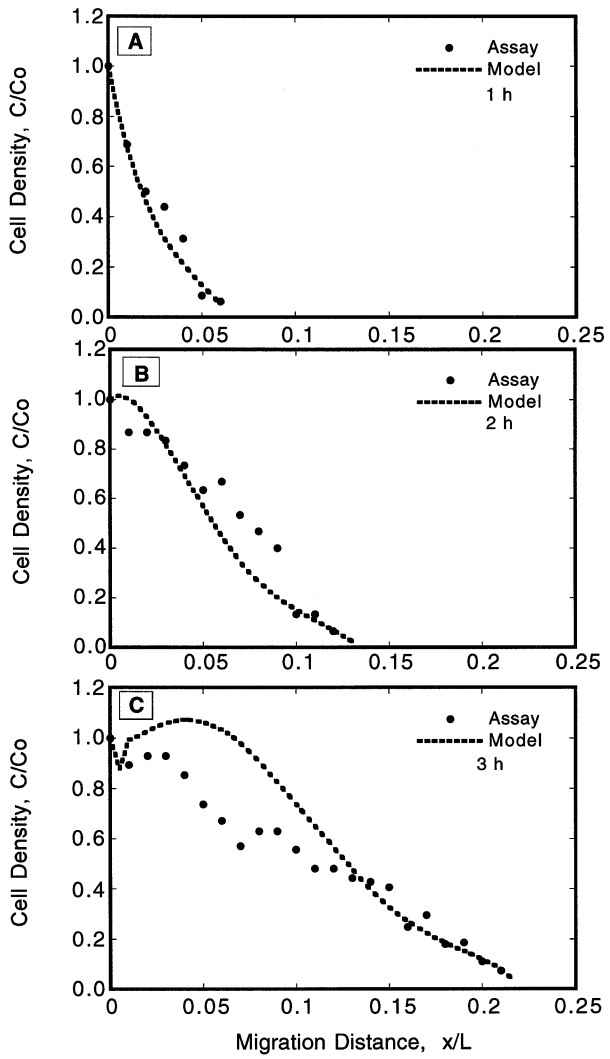

Figure 4 Comparison of experimental (solid lines) and predicted (dashed lines) cell density profiles following chemotaxis at time = 1 h (A), 2 h (B), and 3 h (C) along FMLP concentration gradient established from the right. The initial chemoattractant concentration in the well was 1×10^{-7} M.

every time point, based on the observation that FMLP concentration did not vary significantly across the migration profile. However, the dependence of χ on FMLP concentration was explicitly allowed by admitting different values of χ for every time period of observation, since FMLP concentration values did change significantly between successive hourly time increments. We report that the average χ values changed weakly, as follows: $\chi = 117\,\text{cm}^2/\text{s-M}$ $(a = 6.4 - 8.2 \times 10^{-9}\,\text{M})$; $\chi = 86.5\,\text{cm}^2/\text{s-M}$ $(a = 1.9 - 2.4 \times 10^{-8}\,\text{M})$; and $\chi = 94\,\text{cm}^2/\text{s-M}$ $(a = 2.9 - 3.8 \times 10^{-8}\,\text{M})$.

3.3. Leukocyte chemosensory migration on protein treated ePTFE

Additional experiments were conducted to quantitatively examine the effect of plasma protein adsorption to ePTFE on FMLP-activated leukocyte chemosensory migratory behavior.

In the absence of any FMLP stimulation, the random migratory behavior of PMN on albumin adsorbed ePTFE was slightly higher than on native ePTFE surfaces, and both conditions elicited a significantly higher migration

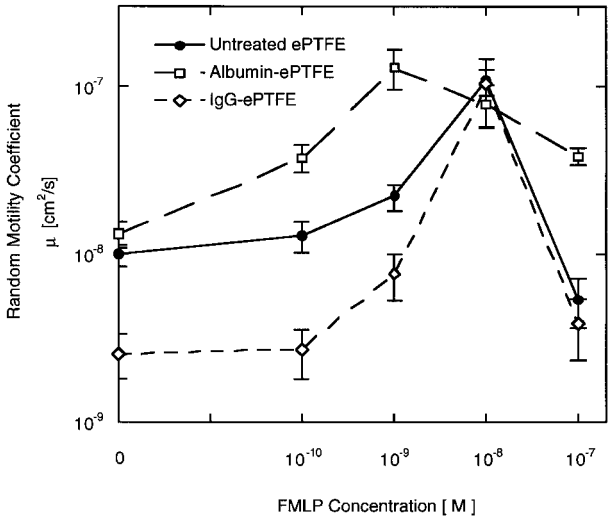

Figure 5 Dependence of the random migration coefficient, μ, on FMLP concentration for various protein pretreated ePTFE conditions.

rate than that observed on IgG adsorbed ePTFE surface, $P < 0.05$ (Fig. 5). Although the qualitative behavior of the μ versus FMLP concentration profiles on protein adsorbed ePTFE was similar to that observed on untreated, native ePTFE, there were several quantitative differences. A primary, protein-specific migratory characteristic was that the value of μ on albumin adsorbed ePTFE was maximized at 10^{-9} M FMLP while that on IgG adsorbed ePTFE was maximized at 10^{-8} M FMLP. Further, on albumin absorbed surfaces, the values of motility coefficient were significantly higher than those on both native and IgG-coated surfaces over a wide range of FMLP concentration, except at the 10^{-8} M FMLP, where μ values were maximized for both native and IgG-coated ePTFE. Additionally, the adsorption of IgG was found to most severely suppress the random migration coefficient in relation to the migration levels elicited by native ePTFE surfaces, with the exception of a very narrow range of FMLP stimulation on IgG around 10^{-8} M FMLP.

In response to a concentration gradient of FMLP, the leukocyte migratory behavior was uniquely altered by the nature of proteins adsorbed to ePTFE surfaces. As shown in Fig. 6, at the 1 h time point (where FMLP concentration was $\sim 0.7 \times 10^{-8}$ M across the distance migrated), the PMN on albumin absorbed surface had a significantly higher chemotaxis coefficient, χ, compared to those on IgG adsorbed ePTFE and untreated ePTFE. Upon increasing the time of incubation to 3 h (whereupon the average FMLP concentration rose six-fold to about 4×10^{-8} M), the PMN chemotactic index on IgG-treated ePTFE increased almost five-fold to 225 $\text{cm}^2/\text{s-M}$, while the χ value on albumin-treated ePTFE decreased from 190 $\text{cm}^2/\text{s-M}$ to 70 $\text{cm}^2/\text{s-M}$. Notably, no statistically significant differences in χ value could be detected for all three conditions at the intermediate time point.

4. Discussion

The objective of this study was to develop a new methodology to determine the motility behavior of leukocytes on the surfaces of implantable, vascular

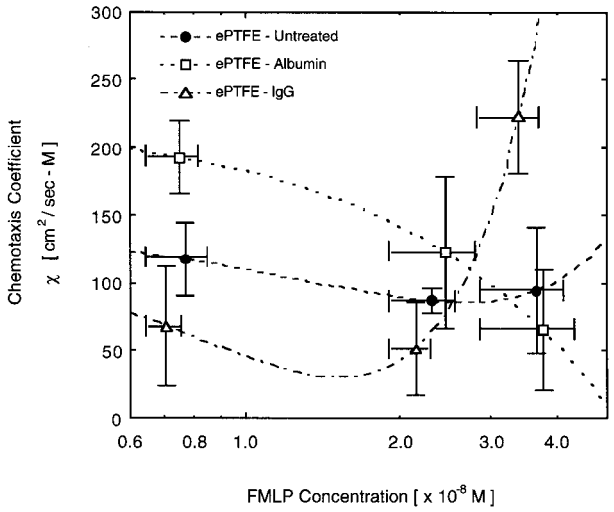

Figure 6 Chemotaxis coefficient profiles for protein coated surface at various averaged values of FMLP concentration (corresponding to 1, 2 and 3 h). The control surface was untreated ePTFE. The horizontal and vertical bars respectively show the range of variation in FMLP concentration and chemotaxis coefficient across the *entire* migration front for each incubation of three independent experiments.

prosthetic biomaterials, and to examine the effect of adsorption of specific plasma proteins on the biomaterial.

Studies of PMN migration on biomaterials have typically been conducted *ex situ*, after cells are flushed following a transient incubation [14]. In contrast, we studied leukocyte migration on ePTFE surfaces *in situ*, using a ''biomaterial-cell-gel'' sandwich configuration, which allows the indirect tracking of population level migration profiles of biomaterial-adherent PMN sandwiched between a gelatin-agar composite gel and an ePTFE membrane. Notably, the cell migration characterized using this method is necessarily in response to continuous cellular biomaterial ''stimulation''. The design of an overlaid gel in this assay is similar to the ''under-agarose'' chemosensory migration technique [15], and thus, using an isotropic field or a gradient field of specific chemokine spatially within the gel, allows the study of either random or directed (chemotactic) modes of PMN migration. The major advantage of this approach is that it allows, via an established theory [17], the measurement of objective, population averaged cell migratory coefficients, μ and χ. These coefficients respectively describe the kinetics of random migration (in response to a uniform chemoattractant field) and chemotaxis (in response to a chemoattractant gradient field). Although these parameters are phenomenologically derived from a probabilistic description for population cell movement [24], they can also be defined in terms of fundamental parameters of individual cell migration. For example, μ is the cellular equivalent of a diffusion coefficient for a molecule, and can be expressed in terms of cell speed, S, and P, the characteristic time before which a cell changes its direction ($\mu = 1/2 \cdot P \cdot S^2$). The directional migration can be characterized by χ, the flux of the population in a given direction, and can be considered as the product of the cell velocity and a parameter related to the average orientation of cells in the gradient. Unlike traditional subjective measurement of cell migration, these parameters are objective measures of migration and reflect the intrinsic cell behavior without ambiguous dependencies on the cell number, duration or geometry of the assay [21]. Thus, the technique proposed here could be potentially useful as a scientific and clinical standard for the evaluation of blood cell migration on prosthetic materials.

Based on our studies of human polymorphonuclear leukocyte migration on ePTFE using the sandwich migration assay, we have reported that microporous vascular prosthetic surfaces such as ePTFE do elicit detectable levels of PMN migration, with the random migration coefficient (μ) ranging from 5.40×10^{-9} to $1.09 \times 10^{-7}\,\mathrm{cm}^2/\mathrm{sec}$, depending on the concentration of chemoattractant, FMLP. While the μ versus FMLP profile obtained on ePTFE was similar to those documented in previous studies [17, 25], the μ values we observed on ePTFE were one order of magnitude lower in the value than to those previously reported for human PMNs on smooth, non-porous, tissue culture plastic (polystyrene) [20]. We suggest that lower μ values on microporous ePTFE may result primarily because the biomaterial surface with 30 μm internodular porosity is tortuous. In our system, the measured extent of migration is essentially a two-dimensional projection of an ''n_D'' dimensional trajectory of migration (where $2 < n_D < 3$). For n-dimensional migration, $\mu = 1/n_D \cdot P \cdot S^2$ [26]; thus, μ depends very sensitively on the cell speed, S, and less strongly on persistence time, P. Thus, assuming that P values do not change significantly (since the material fibers are much wider than the cell size), we propose that the lower μ values may be primarily due to lower migration speed (S), and secondarily due to a higher n_D.

Our studies of PMN chemotaxis on ePTFE suggest that the microporous biomaterial may also cause impaired chemotactic migration. Overall, the range of chemotaxis coefficient values (χ) ranged from 94 to $112\,\mathrm{cm}^2/\mathrm{sec\text{-}M}$ on native ePTFE surface and was less than a third of the maximal χ value reported previously on 2-D, non-porous, tissue culture polystyrene [20]. Lower values of cell speed, S, and χ may indicate a fundamentally different molecular basis for cellular adhesion to ePTFE. For instance, candidate molecules such as leukocyte β_2 integrins are thought likely to mediate PMN adhesion to vascular prosthetic materials [27]. We are currently investigating the role of specific adhesion receptors to ePTFE in modulating PMN migration in a chemoattractant environment [28].

Our results also demonstrate that leukocyte migratory behavior on ePTFE as well as its responsiveness to FMLP activation can be uniquely modulated by adsorbed protein components of plasma, such as albumin and IgG. For example, the ''basal'' μ values on IgG were much lower than those on albumin and untreated ePTFE. Since IgG is one of the most abundant and stable components of plasma, our findings suggest that leukocytes adhering to implanted ePTFE may indeed be poorly motile in the absence of a chemoattractant microenvironment. On IgG-ePTFE, PMN have an extremely high degree of spreading in the absence of FMLP [7], which may limit their ability to migrate. However, FMLP stimulation at specific concentration ($\sim 10^{-8}\,\mathrm{M}$) may lead to marked

induction of morphologic polarity near the ePTFE interface [7], which may explain the significantly higher μ values on IgG seen under these conditions. In contrast to poor migration on IgG-ePTFE, basal migration levels on albumin-ePTFE were comparable to those on ePTFE. This is somewhat surprising since we and others have previously shown that leukocytes on albumin-ePTFE are rounded and weakly polarized [6, 7]. It is possible that the contracted PMN morphology on albumin-eTPFE facilitates migration to occur with minimal interference from the texturally rough surface, while hyperspreading seen on ePTFE or IgG-ePTFE may limit rapid polarization. Migration levels on albumin-ePTFE were also consistently higher than those on ePTFE at most FMLP concentrations; notably, μ on albumin-ePTFE was maximized at an FMLP concentration, which was an order of magnitude lower than that eliciting maximal migration on untreated ePTFE. We have previously shown that FMLP activation progressively enhances PMN spreading near the ePTFE interface as well as its overall morphologic polarity or asymmetry [7]. On albumin-treated ePTFE, PMN adhesion is primarily mediated via CD43, an anti-spreading PMN receptor, that arrests PMN polarization and spreading [29]. Furthermore, the effect of CD43 has been reported to be reversed by the addition of a chemoattractant [29], consistent with our findings that PMN migration is promoted on albumin following FMLP stimulation.

Finally, we have reported that in the chemoattractant concentration range studied, leukocyte chemotactic sensitivity to FMLP can also be markedly altered by the protein adsorption on ePTFE. Albumin and IgG adsorption were found to elicit opposite trends in $\chi(a)$. In fact, the chemotactic mobility, χ times a (cm^2/s), was found to be fairly invariant on albumin, but showed a sharp elevation on IgG and a modest increase on untreated ePTFE surface. Thus, the ratio of directional to random migration, $(\chi a/\mu)$ varied weakly with FMLP concentration on albumin-ePTFE, but increased steeply with increased FMLP concentration (Fig. 7). These findings may have several possible implications for the access of leukocytes to infected implanted biomaterial surfaces. One plausible scenario is that IgG-localized implants may promote the relative directional accuracy of leukocytes ''homing'' toward sites of infection (approaching regions of higher chemoattractant concentration), whereas albumin-rich regions will likely not promote leukocyte directional accuracy. Yet, interestingly, the μ values (at shallow FMLP concentration) are lower on IgG than on albumin, so it is likely that cellular access may be fundamentally limited on IgG owing to the weaker basal signal for the onset of cellular migration. The overall access of leukocytes to infected graft regions will thus be a combined, temporally and spatially regulated result, of both basal migration (μ) and directed migration $(\chi \cdot a)$. It should be noted that $\chi \cdot a/\mu$ is expected to exhibit a biphasic dependence of a, and as such, at much higher values of a (for example, near the source of an infection), the directional motility will be suppressed [20].

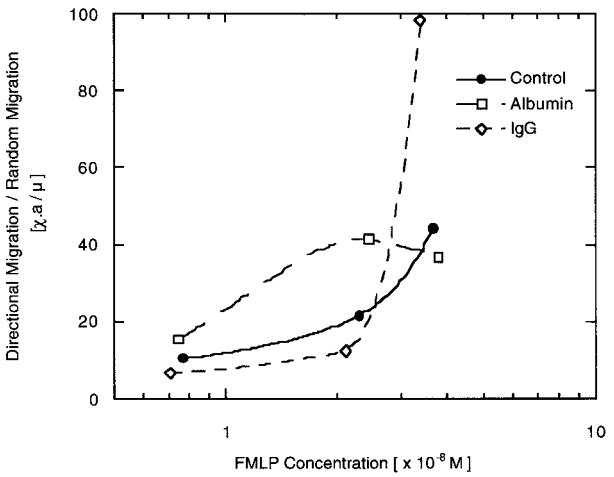

Figure 7 Plot of the ratio of directional motility to random migration, $\chi \cdot a/\mu$, as a function of FMLP concentration, on various protein-treated ePTFE conditions. The control surface was untreated ePTFE.

In summary, we have developed a novel methodology for the evaluation of leukocyte migration on vascular biomaterials, *in situ*. Our results suggest that there is a significant reduction in the migration speed of leukocytes on ePTFE, which may possibly be one of the steps limiting leukocyte bactericidal activity. Previous studies have shown, in fact, that the risk of infection is higher with porous materials than with non-porous materials [1, 30, 31]. We have also shown that specific protein association with ePTFE can strongly enhance both the random and directional components of leukocyte chemosensory migration.

5. Conclusions

Microporous prosthetic biomaterials such as ePTFE suppress the rate of random migration of adherent white blood cells (neutrophilic leukocytes) relative to those reported on 2–D tissue culture substrates. Rates of leukocyte directional migration (chemotaxis), however, are only marginally suppressed, suggesting that the dominantly polarized cells in a chemoattractant gradient may more effectively navigate material surface irregularities. The nature of plasma protein adsorbed to ePTFE can significantly alter both the basal and chemosensory leukocyte migratory response. Albumin promoted overall migratory speed at the expense of directional accuracy, whereas IgG suppressed migration while promoting chemotactic sensitivity at higher chemoattractant concentration.

Acknowledgments

This study was supported by the Whitaker Foundation Biomedical Engineering Research Grant and the Charles & Johanna Busch Biomedical Research Award to Prabhas Moghe. Charlie Chang was partially supported by the Rutgers/UMDNJ NIH Biotechnology Training Program. The generous donation of ePTFE from W. L. Gore & Associates, Inc., is sincerely appreciated.

References

1. K. MERRITT, J. W. SHAFER and S. A. BROWN, *J. Biomed. Mater. Res.* **13** (1979) 101.

2. K. MERRITT, V. M. HITCHINS and A. R. NEALE, *ibid.* **44** (1999) 261.
3. S. D. ELEK and P. D. CONEN, *Br. J. Exp. Pathol.* **38** (1957) 573.
4. D. J. BHAT, V. A. TELLIS, W. I. KOHLBERG, B. DRISCOLL and F. J. VEITH, *Surgery* **87** (1980) 445.
5. S. H. DOUGHERTY and R. L. SIMMONS, *Curr. Problems Surg.* **19** (1982) 289.
6. D. A. KATZ, B. HAIMOVICH and R. S. GRECO, *Surgery* **116** (1994) 446.
7. C. C. CHANG, S. M. LIEBERMAN and P. V. MOGHE, *Biomaterials* **20** (1999) 273.
8. P. SWARTBOL, L. TRUEDSSON, H. PARSSON and L. NORGREN, *J. Biomed. Mater. Res.* **32** (1996) 669.
9. M. B. GORBET, E. L. YEO and M. V. SEFTON, *ibid.* **44** (1999) 289.
10. W. ZIMMERLI, F. A. WALDVOGEL, P. VAUDAUX and U. E. NYGEGGER, *J. Infections Diseases* **146** (1982) 487.
11. A. FINN, N. MOAT, N. REBUCK, N. KLEIN, S. STROBEL and M. ELLIOTT, *Agents Actions* **38** (1993) C44.
12. J. P. CRISTOL, B. CANAUD, H. RABESANDRATANA, I. GAILLARD, A. SERRE and C. MION, *Nephrol Dial Transplant* **9** (1994) 389.
13. S. S. KAPLAN, R. E. BASFORD, R. L. KORMOS, R. L. HARDESTY, R. L. SIMMONS, E. M. MORA, M. CARDONA and B. L. GRIFFITH *ASAIO Transactions* **36** (1990) M172.
14. A. PIZZOFERRATO, A. VESPUCCI, G. CIAPETTI and S. STEA, in ''Techniques of Biocompatibility Testing'' edited by D. F. Williams (CRC Press, Inc., Boca Raton, 1986), vol. II, pp. 109.
15. R. D. NELSON, P. G. QUIE and R. L. SIMMONS, *J. Immunol.* **118** (1975) 1650.
16. J. E. CUTLER, *Proc. SO. Exp. Biol. Med.* **147** (1974) 471.
17. D. A. LAUFFENBURGER, C. ROTHMAN and S. H. ZIGMOND, *J. Immunol.* **131** (1983) 940.
18. J. D. ANDRADE and V. HLADY, *Ann. New York Acad. Sci.* **516** (1987) 158.
19. A. FERRANTE and Y. H. THONG, *J. Immunological Methods* **36** (1980) 109.
20. R. T. TRANQUILLO, S. H. ZIGMOND and D. A. LAUFFENBURGER, *Cell Motility and the Cytoskeleton* **11** (1988) 1.
21. D. A. LAUFFENBURGER, *Agents Actions* [Suppl.] **12** (1983).
22. M. ABRAMOWITZ and L. A. STEGUN, ''Handbook of Mathematical Functions'' (Dover Press, New York, 1965).
23. A. CONSTANTINIDES, ''Applied Numerical Methods with Personal Computers'' Chemical Engineering Series (McGraw-Hill, New York, 1987).
24. W. ALT, *J. Math. Biol.* **9** (1980) 147.
25. H. M. BUETTNER, D. A. LAUFFENBURGER and S. H. ZIGMOND, *AlChE J.* **35** (1989) 459.
26. G. A. DUNN, in ''Biology of the Chemotactic Response'' edited by J. M. Lacke and P. C. Wilkinson (Cambridge University, Cambridge, 1981) p. 1.
27. L. BENTON, U. PUROHIT, M. KHAN and R. GRECO, *J. Surgical Res.* **64** (1996) 116.
28. C. C. CHANG, R. S. SCHLOSS, T. D. BHOJ and P. V. MOGHE, *J. Biomed. Mater. Res.* (submitted) (1999).
29. C. NATHAN, Q. XIE, L. HALBWACHS-MECARELLI and W. W. JIN, *J. Cell Biology* **122** (1993) 243.
30. J. CORDERO, L. MUNUERA and M. D. FOLGUEIRA, *J. Bone Joint Surg.* **76B** (1994) 717.
31. J. W. ALEXANDER, J. Z. KAPLAN and W. A. ALTEMEIER, *Ann. Surg.* **165** (1967) 192.

Received 23 April 1999
and accepted 14 September 1999